CALIBRATION OF A SIX-PORT POSITION SENSOR VIA SUPPORT VECTOR REGRESSION

H. Peng[*], T. Yang, and Z. Q. Yang

School of Electronic Engineering, University of Electronic Science and Technology of China, Chengdu, Sichuan 611731, P. R. China

Abstract—In this paper, a calibration technique for the position sensor via support vector regression (SVR) is proposed. The position sensor adopts a zero-intermediate frequency architecture based on a six-port network, which is used for directly measuring the phase differences and indirectly reflecting the position. The SVR, which implements the structural risk minimization (SRM) principle, provides a good generalization ability from size-limited data sets. The results indicate that the SVR model can achieve a great predictive ability in positioning, with an accuracy of 2.41 mm over a distance range of 274.5 mm.

1. INTRODUCTION

Engen and Hoer made an early research of the six-port technique in 1972 [1]. The researchers then found that the six-port technique could be used for communication transceivers [2–4], direction finding receivers [5] and ranging receivers [6–9], etc.

Ranging is a fundamental function of a radar system and plays an extremely important role in electronic warfare. Several studies on the position sensor using the six-port technique have been reported [6–9]. In these papers, the researchers mainly used the frequency modulation continuous wave (FMCW) [6–8] or two adequately spaced continuous wave (CW) frequencies [9] to measure the position. The advantages of a position sensor based on the six-port technique are as follows: operation in millimeter wave frequencies, no mixer, low-power consumption, implementation in MMIC (low-cost and compact size), etc. As such, this receiver architecture has been adopted in the modern radar systems. However, because of the asymmetry of

the six-port junctions and the nonlinearity of the diode detectors, the calibration technique of a position sensor has to be carefully considered. A calibration method based on a sample data set, such as the artificial neural network (ANN), is applied in the six-port network for non-linear approximation [10]. However, the ANN method can cause over-fitting, produce multiple local minimum solutions, and have low generalization ability [11].

The earliest study on the support vector machine (SVM) theory was reported in 1995 by Vapnik [12]. The SVM theory has been successfully used in classification and regression problems [13–15]. SVM embodies the structural risk minimization (SRM) principle instead of the traditional empirical risk minimization (ERM) which is applied in the ANN. SVMs can solve a constrained quadratic optimization problem (in contrast to the multi-extremal minimization in the ANNs), and are based on the small-sample statistical learning theory, which allows the control of the generalization ability and its model's complexity [16]. Therefore, SVM can always find a global minimum.

In previous studies, the accuracy of the position sensor was mainly related to the accuracy of the measured phase differences attributed to the asymmetry of six-port junctions, the nonlinearity of diode detectors, and other factors. A calibration technique for six-port networks was proposed [10], and its operating frequency was set at a fixed value. In this work, the range of operating frequency is set within the 5 GHz to 6 GHz. A calibration technique based on the support vector regression (SVR) method for the position sensor is proposed. The input data of the SVR model are I/Q voltages, whereas the output data are the distances. The principle of the position sensor is introduced, and an example of distance calibration based on the SVR model is given to demonstrate its effectiveness.

2. OPERATING PRINCIPLE

The six-port network was proven to be a suitable architecture for position sensors according to phase difference measurements [9, 17], which have a close relationship with the relative amplitudes of the I/Q signals. A six-port network is used to determine the distance from the antennas to the target. Figure 1 shows the block diagram of a position sensor.

The position sensor includes two separated antennas, a LNA, a six-port junction, four detectors, and two differential amplifiers, and other devices. One of the outputs of the coupler outputs is injected into the transmitting antenna, and the other one is injected into the
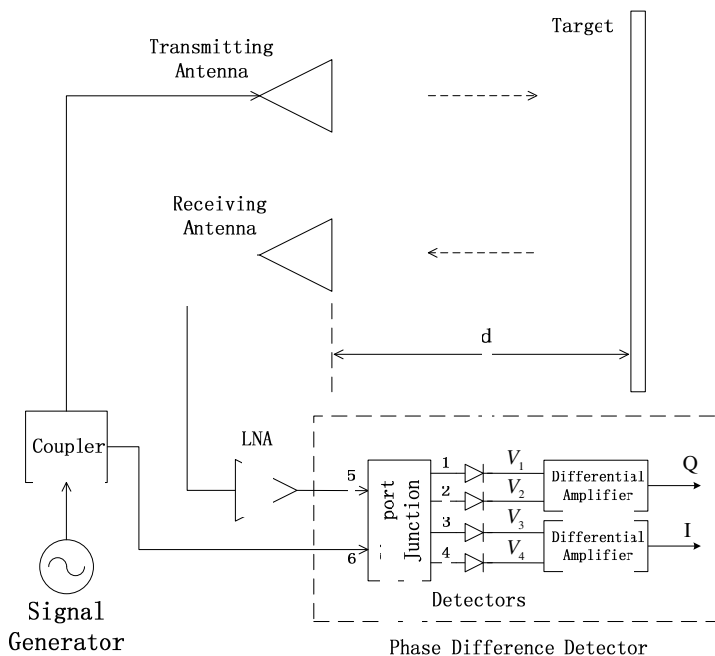
Figure 1. Block diagram of a position sensor.

phase difference detector module. Two separate antennas are used to reduce the crosstalk between the transmitted and received microwave signals and to simplify the system.

Figure 2 shows the block diagram of the six-port junction circuit, composed of a Wilkinson power divider and three 90° hybrid couplers [18].

In order to obtain the output signals, four power detectors are connected to the six-port junction outputs. The output voltage of the ideal power detector is proportional to the square magnitude of the RF input signal.

$$V_i = K_i \left| b_i \right|^2, \quad i = 1, 2, 3, 4 \tag{1}$$

where K_i constants are measured in V/W.

Supposing that four identical detectors $K_i = K$ and four low-pass filters are used, the output voltages can be expressed as follows:

$$V_i = \frac{K}{4} \left[A^2 + B^2 + 2A \cdot B \cdot (-1)^i \cdot \cos(\phi - j \cdot \pi/2) \right]$$

$$\begin{cases} j = 0, & \text{if } i = 1, 2 \\ j = 1, & \text{if } i = 3, 4 \end{cases} \tag{2}$$

$$b_2 = \frac{1}{2}(a_5 + a_6) \qquad b_1 = -\frac{j}{2}(a_5 - a_6)$$

$\leftarrow$ 90° hybrid couplers

$-j\dfrac{a_5}{\sqrt{2}}$ $\qquad \dfrac{a_6}{\sqrt{2}}$ $\qquad \downarrow$ $\qquad Z_0$

$a_5 = A\cos(\omega t)$

Power divider $\qquad -j\dfrac{a_5}{\sqrt{2}}$ $\qquad j\dfrac{a_6}{\sqrt{2}}$ $\qquad a_6 = B\cos(\omega t + \phi)$

$\leftarrow$ 90° hybrid couplers

$$b_3 = \frac{1}{2}(a_5 + ja_6) \qquad b_4 = -\frac{j}{2}(a_5 - ja_6)$$
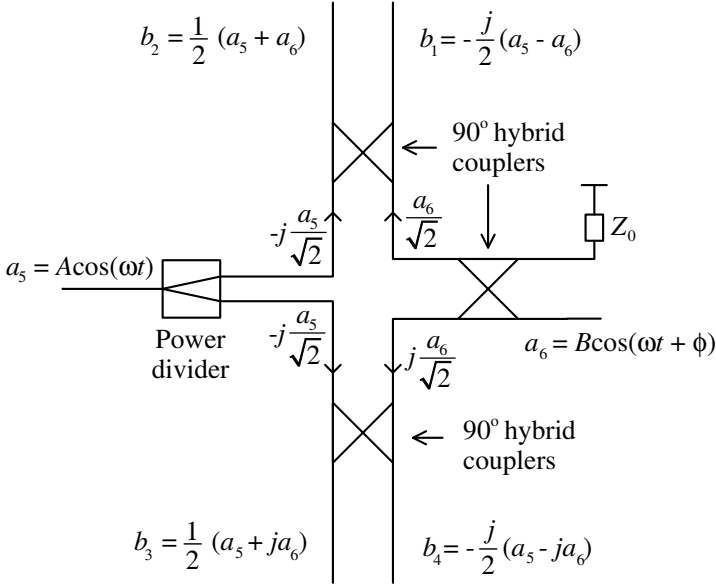
Figure 2. Block diagram of the six-port junction circuit.

$$\phi = \tan^{-1}\left(\frac{V_4 - V_3}{V_2 - V_1}\right) \tag{3}$$

where V_i are the output voltages of the detectors, K is the constant factor, A and B are the amplitudes of the two input signals of the six-port junction, i is the correlator output port index, and ϕ is the phase difference between the two injected signals of the six-port junction.

The relationship between the distance, the frequency difference, and the phase difference can be expressed as follows [9]:

$$d = \frac{c(\phi_2 - \phi_1)}{4\pi(f_2 - f_1)} = \frac{c(\phi_2 - \phi_1)}{4\pi \cdot \Delta f} \tag{4}$$

where d is the distance to the target, c is the speed of light, ϕ_2 is the corresponding phase of f_2, and ϕ_1 is the corresponding phase of f_1. The maximum unambiguous distance for $\phi_2 - \phi_1 = 2\pi$ can be determined using Equation (4).

The maximum unambiguous distance is inversely proportional to the frequency difference. In engineering practice, Δf could be a reasonable choice based on the maximum unambiguous distance. In this work, to facilitate the experiment set-up in anechoic chamber, a $\Delta f = 500\,\text{MHz}$ frequency difference gives a maximum unambiguous distance of 300 mm.

The distance to the target d appears simple. However, many factors can introduce inaccuracies, including six-port junction errors, detector inconsistencies and nonlinearities, changes in the transmission phase in LNA if the input power is changed, and mismatches due to the source and load, among others. Therefore, Equation (4) can be expressed as follows:

$$d = f\left[(V_2 - V_1)_{f_1}, (V_4 - V_3)_{f_1}, (V_2 - V_1)_{f_2}, (V_4 - V_3)_{f_2}\right] \qquad (5)$$

where $f(\cdot)$ is a real nonlinear function, the explicit function of which is impossible to obtain.

A fixed Δf means a fixed maximum unambiguous distance. When Δf is a constant value, the frequencies f_1 and f_2 can be set at the operating frequency band. From another perspective, a larger amount of phase difference information, which has a strong intrinsic relationships, means obtaining a higher positioning accuracy. Hence, Equations (4) and (5) can be rewritten as follows:

$$d = \frac{c(\phi_m - \phi_n)}{4\pi(f_m - f_n)} \quad m, n = 1, 2, 3 \ldots \qquad (6)$$

$$\begin{aligned}
d = {}& g\left[(V_2 - V_1)_{f_1}, (V_4 - V_3)_{f_1}, (V_2 - V_1)_{f_2}, (V_4 - V_3)_{f_2} \ldots \right. \\
& \left. (V_2 - V_1)_{f_m}, (V_4 - V_3)_{f_m}, (V_2 - V_1)_{f_n}, (V_4 - V_3)_{f_n} \ldots\right] \qquad (7)
\end{aligned}$$

where $g(\cdot)$ is a nonlinear complex function.

An excessive training data set results in overtraining and overly complicates the SVR model. To improve the positioning accuracy and simultaneously control the size of the training data set, the frequencies $f_1 = 5\,\text{GHz}$, $f_2 = 5.5\,\text{GHz}$ and $f_3 = 6\,\text{GHz}$ are chosen. Therefore, the distance to the target d can be expressed as:

$$\begin{aligned}
d = {}& \frac{c(\phi_2 - \phi_1)}{4\pi(f_2 - f_1)} = \frac{c(\phi_3 - \phi_2)}{4\pi(f_3 - f_2)} = \frac{c \cdot \Delta\phi}{4\pi \cdot \Delta f} \\
= {}& h\left[(V_2 - V_1)_{f_1}, (V_4 - V_3)_{f_1}, (V_2 - V_1)_{f_2}, (V_4 - V_3)_{f_2}, \right. \\
& \left. (V_2 - V_1)_{f_3}, (V_4 - V_3)_{f_3}\right] \qquad (8)
\end{aligned}$$

where $h(\cdot)$ is a nonlinear complex function.

3. EXPERIMENT AND RESULTS

In this section, a six-port position sensor is used to verify the accuracy of the SVR model. A precision track and a programmable synthesized signal generator (Agilent 83752A) are used. The position sensor consists of two pyramidal horn antennas, one LNA, one six-port junction, one coupler, four detectors, two broadband operation amplifiers, one metal plate, one precision track, and other devices. The
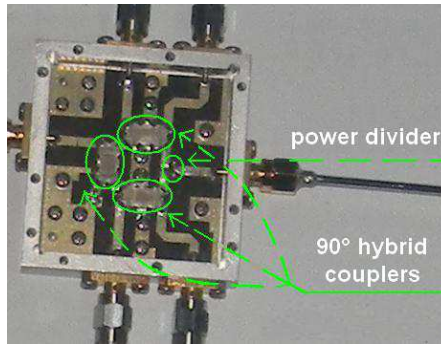
Figure 3. Six-port junction circuit.

six-port junction circuit was realized on Taconic-TLX-8 ($h = 0.79$ mm, $\varepsilon_r = 2.55$). The noise figure of LNA is about 3.5 dB. The output voltages of detectors operating in the square-law region are less than 70 mV. Coupling coefficient of the direction coupler is 10 dB. Figure 3 shows the six-port junction circuit, composed of a power divider and three 90° hybrid couplers.

A pulse signal instead of the CW is used. The input noise amplified by the LNA is directly added to the DC offset output from the detectors. Due to the existence of common mode rejection (CMR) performance of differential operation amplifiers, the asymmetry of the six-port junction and the inconsistency of the diode detectors, the DC offset voltages couldn't be fully cancelled. The DC offset voltages is superimposed on the I/Q output voltages, and can be measured in a pulse signal system. Figure 4 shows the photograph of the six-port position sensor prototype circuit in anechoic chamber.

A metal plate, with a fixed precision track is used to simulate a target. The phase differences of the two signals injected into the six-port network can be changed by using the precision track side. Two pyramidal horn antennas are used as the transmitting and receiving antennas. The gain of the transmitting antenna is greater than 20 dB, and a 3 dB main beamwidth of ±8° is achieved. Meanwhile, the dimension of the receiving antenna aperture is relatively small. Its gain is approximately 17 dB, and the 3 dB main beamwidth is ±10°. The two antennas both have sidelobe levels below −20 dB.

The distances are set from 500 mm to 774.5 mm at approximately 0.5 mm steps, and the frequencies are set from 5 to 6 GHz at 500 MHz steps. In the current work, to facilitate the experiment set-up in anechoic chamber, a starting position is set 500 mm away from the antennas in the far-field region, and a maximum unambiguous distance
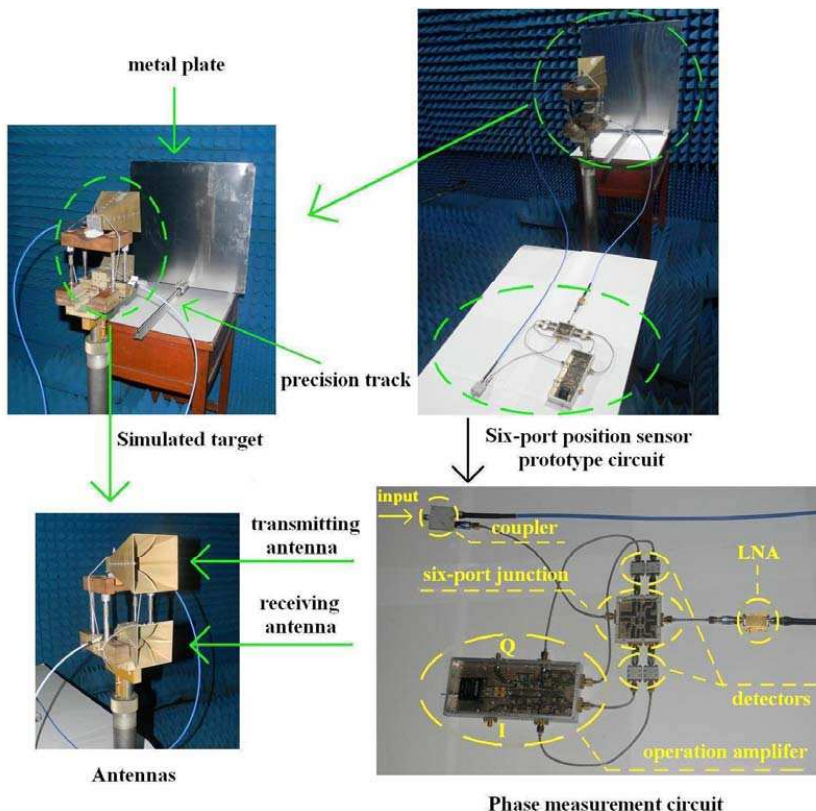
Figure 4. Six-port position sensor prototype circuit in anechoic chamber.

of 300 mm is given based on a $\Delta f = 500\,\text{MHz}$ frequency difference. Therefore the real distances can be uniquely determined by the phase differences in the range of 500 mm to 800 mm. Nevertheless, in order to detect distant targets in a practical system, a decreased frequency difference Δf and a increased maximum unambiguous distance are needed.

All readings on the digital oscilloscope are measured and recorded, and a total of 550 standards are set up. About 60% of the data (350 samples) are randomly selected as the training data set, and the rest are included in the cross-validation data set (200 samples).

The LIBSVM toolbox, which is developed by C. C. Chang and C. J. Lin, is utilized to calculate the various models [19]. The core idea of SVR method was mentioned in [14]. The SVR parameters could be determined before running code: the constant defining of kernel

function (γ), the tolerance of termination criterion (ε), the penalty parameter (C) and the constant ν. $\nu \in [0, 1]$ is the parameter that controls the number of support vectors. The optimal parameters of γ and C can be calculated using the K-fold Cross-Validation (K-CV) method [20]. The SVR parameters are as follows: $\varepsilon = 0.0001$, $\nu = 0.1$, $C = 0.117$, and $\gamma = 0.66$. Moreover, the Root Mean Square Error (RMSE) and the Pearson Product-Moment correlation coefficient (R) are calculated to determine the accuracy of the SVR model. RMSE and R are given as:

$$\text{RMSE} = \sqrt{\frac{1}{N} \sum_{i=1}^{N} (a_i - b_i)^2} \tag{9}$$

$$R = \frac{\sum_{i=1}^{N} \left(b_i - \bar{b}\right)\left(a_i - \bar{a}\right)}{\sqrt{\sum_{i=1}^{N} \left(b_i - \bar{b}\right)^2 \sum_{i=1}^{N} \left(a_i - \bar{a}\right)^2}} \tag{10}$$

where a_i is the predicted distance of the training or cross-validation data set based on the SVR model, $\bar{a}$ is the predicted distance mean of the training or cross-validation data set based on the SVR model, b_i is the distance, $\bar{b}$ is the distance mean, and N is the data number.

Figure 5(a) shows distances against the values predicted by SVR model for the training data set (350 samples). The RMSE of the distance is 2.108 mm over the 500 mm to 774.5 mm range. The fresh cross-validation data set (200 samples) is used for determining the accuracy of the proposed SVR model. Figure 5(b) shows the distances
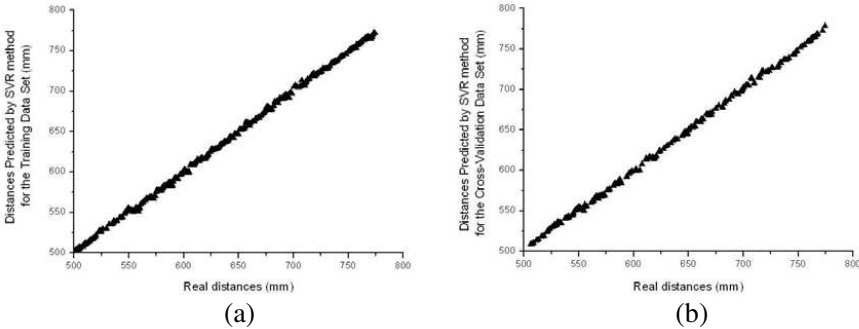
Figure 5. Measured and calibrated results: (a) distances versus the values predicted by SVR model for the training data set (350 samples) and (b) distances versus the values predicted by SVR model for the cross-validation data set (200 samples).

Table 1. RMSE and R of the training and cross-validation data sets.

	Training Data Set (350 samples)	Cross-Validation Data Set (200 samples)
RMSE	2.108 mm	2.410 mm
R	0.9997	0.9995
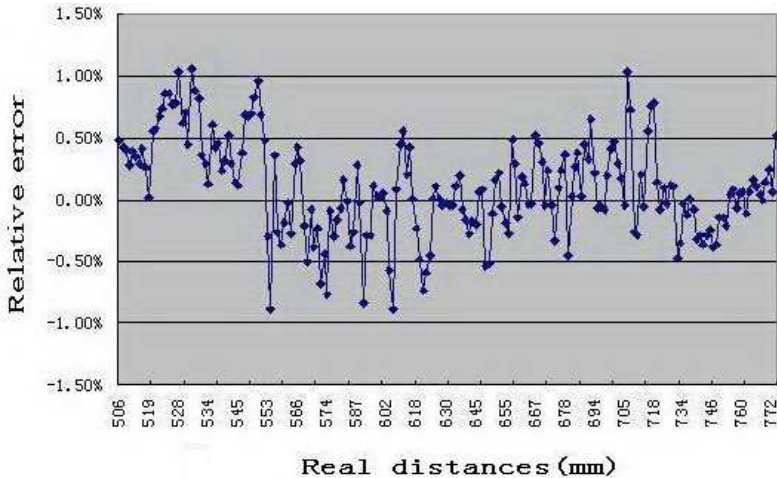
Figure 6. Relative errors versus real distances.

against the values predicted by SVR model for the cross-validation data set. The RMSE of the distance is 2.41 mm over the 500 mm to 774.5 mm range. These results are summarized in Table 1 and show that the SVR model predicts the results well.

Figure 6 shows the relative errors versus real distances and indicates that the relative errors of most predicted results are less than ±1%.

4. CONCLUSION

The positioning accuracies in previous studies mainly relied on the hardware characteristics, such as the six-port junction symmetry, detector consistencies, and ignored the software calibration technique. In the current work, a calibration technique based on the SVR model is introduced into the six-port position sensor without necessarily considering the physical properties of the modules and the components. In [9], the target was situated at around 700 cm, and a mean of the measured distance to the target was 729 cm. A mean error of

approximately 4% was obtained. In this work, the changed range of the distance is 274.5 mm (500 mm to 774.5 mm), and the calibration achieves an RMSE of 2.41 mm. Based on the calibration of SVR method, the relative errors of most predicted results are less than ±1%.

ACKNOWLEDGMENT

REFERENCES

1. Engen, G. F. and C. A. Hoer, "Application of an arbitrary 6-port junction to power-measurement problems," *IEEE Trans. Instrum. Meas.*, Vol. 21, No. 4, 470–474, Nov. 1972.

2. De la Morena-Álvarez-Palencia, C. and M. Burgos-Garcia, "Four-octave six-port receiver and its calibration for broadband communications and software defined radios," *Progress In Electromagnetics Research*, Vol. 116, 1–21, 2011.

3. Khaddaj Mallat, N., E. Moldovan, and S. O. Tatu, "Comparative demodulation results for six-port and conventional 60 GHz direct conversion receivers," *Progress In Electromagnetics Research*, Vol. 84, 437–449, 2008.

4. Zhao, Y., C. Viereck, J. F. Frigon, R. G. Bosisio, and K. Wu, "Direct quadrature phase shift keying modulator using six-port technology," *Electronics Letters*, Vol. 41, No. 21, 1180–1181, Oct. 2005.

5. Yakabe, T., F. Xiao, K. Iwamoto, F. M. Ghannouchi, K. Fujii, and H. Yabe, "Six-port based wave-correlator with application to beam direction finding," *IEEE Trans. Instrum. Meas.*, Vol. 50, No. 2, 377–380, Apr. 2001.

6. Boukari, B., E. Moldovan, S. Affes, K. Wu, R. G. Bosisio, and S. O. Tatu, "A heterodyne six-port FMCW radar sensor architecture based on beat signal phase slope techniques," *Progress In Electromagnetics Research*, Vol. 93, 307–322, 2009.

7. Boukari, B., E. Moldovan, S. Affes, K. Wu, R. G. Bosisio, and S. O. Tatu, "A 77 GHz six-port FMCW collision-avoidance radar sensor with baseband analytical calibration," *Microw. Optical Technology Lett.*, Vol. 51, No. 3, 720–725, 2009.

8. Stelzer, A., C. G. Diskus, K. Luebke, and H. W. Thim, "A microwave position sensor with submillimeter accuracy," *IEEE*

Transactions on Microwave Theory and Techniques, Vol. 47, No. 12, 2621–2624, 1999.

9. Moldovan, E., S. O. Tatu, T. Gaman, K. Wu, and R. G. Bosisio, "A new 94 GHz six port collision avoidance radar sensor," *IEEE Transactions on Microwave Theory and Techniques*, Vol. 52, No. 3, 751–759, 2004.

10. Liu, Y., "Calibrating an industrial microwave six-port instrument using the artificial neural network technique," *IEEE Trans. Instrum. Meas.*, Vol. 45, No. 2, 651–656, Apr. 1996.

11. Chen, K., C. Ho, and H. Shiau, "Application of support vector regression in forecasting international tourism demand," *Tourism Management Research*, Vol. 4, 81–97, 2004.

12. Vapnik, V., *The Nature of Statistical Learning Theory*, Springer-Verlag, New York, 1995.

13. Wei, C., J. O. Chong, and S. S. Keerthi, "An improved conjugate gradient scheme to the solution of least squares SVM," *IEEE Trans. Neural Network*, Vol. 6, 498–501, 2005.

14. Xia, L., R.-M. Xu, and B. Yan, "LTCC interconnect modeling by support vector regression," *Progress In Electromagnetics Research*, Vol. 69, 67–75, 2007.

15. Yang, Z. Q., T. Yang, Y. Liu, and S. H. Han, "MIM capacitor modeling by support vector regression," *Journal of Electromagnetic Waves and Applications*, Vol. 22, No. 1, 61–67, 2008.

16. Bermani, E., A. Boni, A. Kerhet, and A. Massa, "Kernels evaluation of SVM-based estimators for inverse scattering problems," *Progress In Electromagnetics Research*, Vol. 53, 167–188, 2005.

17. Li, J., R. G. Bosisio, and K. Wu, "A collision avoidance radar using six-port phase/frequency discriminator," *IEEE MTT-S International Microwave Symposium*, 1553–1556, 1994.

18. Tatu, S. O., E. Moldovan, K. Wu, R. G. Bosisio, and T. A. Denidni, "Ka-band analog front-end for software-defined direct conversion receiver," *IEEE Transactions on Microwave Theory and Techniques*, Vol. 53, 2768–2776, 2005.

19. Chang, C. C. and C. J. Lin, "LIBSVM: A library for support vector machines," System Documention, National Taiwan University, 2004.

20. Bengio, Y. and Y. Grandvalet, "No unbiased estimator of the variance of K-fold cross-validation," *J. Machine Learning Research*, Vol. 5, 1089–1105, 2004.